*Bull. Chem. Soc. Jpn.*, **72**, 1781—1784 (1999)

# Molecular Structure of a $\mu$-Oxo Chromium–Iron Complex: Rare Example of a Crystallographically Characterized $\mu$-Oxo Heterometallic Porphyrin

**Kenichi Oyaizu, Agus Haryono, Yukio Nishimura, Kimihisa Yamamoto,**[#] **and Eishun Tsuchida***, [##]

Advanced Research Institute for Science and Engineering, Department of Polymer Chemistry, Waseda University, Tokyo 169-8555

(Received February 16, 1999)

The crystal structure of a $\mu$-oxo heterometallic porphyrin [(pip)(tpp)$Cr^{III}OFe^{III}$(tpp)] (pip = piperidine) not only confirmed the proposed oxidation state of chromium and iron atoms, but also revealed a unique coordination environment around chromium(III), which is substantially protruded from the porphyrin plane.

Recent interest in the chemistry of oxo-bridged metal complexes ([LM–O–ML], L = ligand) has been stimulated by their significance as multi-electron redox catalysts.[1] A typical example is the $O_2$-oxidative polymerization of diphenyl disulfide catalyzed by a $\mu$-oxo dinuclear vanadium complex under acidic conditions,[2] which provides a convenient synthesis of poly(*p*-phenylene sulfide), an important engineering plastic.[3] We previously reported that a model complex of the catalyst, [$V^{IV}O$(salen)] ($H_2$salen = *N*,*N*′-ethylenebis(salicylideneamine)), is converted to $[V(salen)]^{2+}$ by a reaction with $H^+$.[4] The resulting cation is oxophilic and enters into an equilibrium with [VO(salen)] to form a $\mu$-oxo dinuclear vanadium complex according to

$$[(salen)V{=}O] + [V(salen)]^{2+} = [(salen)V^{IV}OV^{IV}(salen)]^{2+}.$$

On the other hand, the formation of $\mu$-oxo diiron(III) [(porph)$Fe^{III}OFe^{III}$(porph)] (porph = porphyrin dianion) by a reaction of $O_2$ with [(porph)$Fe^{II}$] species proceeds via the formation of a reactive ferryl species [(porph)$Fe^{IV}{=}O$], which gives the oxo-bridged species[5] by the reaction

$$[(porph)Fe^{IV}{=}O] + [(porph)Fe^{II}] \rightarrow [(porph)Fe^{III}OFe^{III}(porph)].$$

Such reactions might be expected to occur between other oxometal species and similar metal complexes in lower oxidation states. Indeed, the reactive [(tpp)$Fe^{IV}{=}O$] (tpp = 5,10,15,20-tetraphenylporphyrin dianion) couples with a copper(I) complex to yield a product considered to be an $Fe^{III}$–O–$Cu^{II}$ species,[6] which has been suggested to provide a model for the active site of cytochrome c oxidase,[7] though the product was not structurally characterized. In a pioneering work by West et al. it was reported that the reaction of a more stable [(porph)$Cr^{IV}{=}O$] species with [(porph)$Fe^{II}$] formed [(porph)CrOFe(porph)], a compound with magnetic properties of interest. However, only preliminary X-ray diffraction data were described due to a difficulty to obtain crystals of the compound.[8] Although $\mu$-oxo heterodinuclear porphyrins are thus of significant interest, only a few studies have been reported on their crystal structures.[9] Here, we describe the molecular structure of a $\mu$-oxo heterometallic porphyrin [X(tpp)$Cr^{III}OFe^{III}$(tpp)] (X = piperidine) and that of a mononuclear analogue [X(tpp)$Cr^{III}$Cl] (X = pyridine), both fully characterized by X-ray crystallography. A comparison of the two structures not only confirms the proposed valence state of the heterodinuclear complex,[8] but also provides additional insight into the unique oxophilic character of iron(II) with possible relevance to heme proteins.

## Experimental

**Materials.** All solvents were purified by distillation. Iodosobenzene, piperidine, $CrCl_2$, $H_2$tpp, and [(tpp)FeCl] were used as received.

**Preparation of [(tpp)CrCl(py)]·$C_6H_{14}$ (py = pyridine) (I).** The chromium(III) complex [(tpp)CrCl] was prepared as previously described[10] with slight modifications. Metalation of $H_2$tpp was conducted in refluxing DMF using anhydrous chromium(II) chloride. The product was purified by crystallization from pyridine–hexane solutions to yield black prismatic crystals. Anal. Calcd for $C_{55}H_{47}N_5CrCl$: C, 76.32; H, 5.47; N, 8.09%. Found: C, 75.99; H, 5.45; N, 8.10%. $D_{obsd} = 1.30\ g\,cm^{-3}$. UV ($\lambda_{max}$, nm, $CH_2Cl_2$) 436, 542.

**Preparation of [(tpp)FeOCr(tpp)(pip)] (pip = piperidine) (II).** The oxochromium(IV) complex [(tpp)Cr=O] was prepared by the oxidation of [(tpp)CrCl] with iodosobenzene.[11] In a typical reaction, [(tpp)CrCl] and iodosobenzene were stirred vigorously in benzene. The resulting dark-red solution was transferred to an alumina column and eluted with benzene. Evaporation of the eluate gave small, dark crystals of [(tpp)Cr=O]. The reduction of [(tpp)FeCl] was performed using piperidine as previously described[12] with slight modifications. The addition of piperidine to a solution of [(tpp)FeCl] in $CH_2Cl_2$ at 40 °C produced [(tpp)$Fe^{II}(pip)_2$], which was purified by recrystallization from methanol. A reaction between [(tpp)Cr=O] and [(tpp)Fe$(pip)_2$] occurred readily in dry toluene under argon to yield the $\mu$-oxo chromium–iron porphyrin.[8] Re-

---

[#] Present address: Department of Chemistry, Keio University.

[##] CREST investigator, JST.

crystallization of the product from benzene-hexane solutions gave black prismatic crystals of **II**. Anal. Calcd for $C_{93}H_{67}N_9OFeCr$: C, 77.86; H, 4.71; N, 8.79%. Found: C, 77.23; H, 4.21; N, 8.60%. UV ($\lambda_{max}$, nm, $CH_2Cl_2$) 431, 546, 571.

**X-Ray Crystallography.** Crystals of **I** were grown from pyridine solutions after layering with hexane, and those of **II** were grown from benzene–diethyl ether. All measurements for **I** were made on a Rigaku AFC7R diffractometer, and for **II** on a Rigaku RAXIS-IV imaging plate area detector with graphite-monochromated Mo $K\alpha$ radiation ($\lambda$ = 0.71073 Å). Unit cell parameters and an orientation matrix for data collection for **I** were determined by least-squares refinements using the setting angles of 25 carefully centered reflections in the range $25.42 < 2\theta < 29.95°$. The data for **I** were collected using the $\omega$–$2\theta$ scan technique to a maximum $2\theta$ value of 55°. The intensities of three representative reflections were measured after every 150 reflections. No decay was observed during the data collection for **I**. Indexing for **II** was performed from three 1.0° oscillation images which were exposed for 4.0 min. The crystal-to-detector distance was 125.0 mm with the detector at the zero swing position. The data for **II** were collected at a temperature of 25 °C to a maximum $2\theta$ value of 50.2°. Completeness of the measurement was 0.68 ($R_{merge}$ = 0.045 for 9977 unique reflections). A total of sixty 3.0° oscillation images were collected, each being exposed for 50.0 min. Readout was performed in the 100 μm pixel mode. When the data for **II** was collected with a point detector, the collection of ca. 16000 points took ca. 8 d, which resulted in a steep decrease in the reflection intensities after ca. 5 d of X-ray irradiation. On the other hand, the collection of data using the area detector took only 50 min/image × 60 = 50 h and virtually no decay was observed during such a short-time irradiation. In addition, the use of highly sensitive imaging plate was effective for collecting weak reflections from the small crystal of **II**.

**Structure Solution and Refinement.** The structures for **I** and **II** were solved by heavy-atom Patterson methods and expanded using Fourier techniques (Scheme 1). For **I**, non-hydrogen atoms in the lattice solvent molecule (hexane) were refined isotropically, while the rest were refined anisotropically. Hydrogen atoms were not included. In spite of the considerable disorder of the solvent molecule, the structure for **I** containing one solvent molecule per Cr(tpp) unit was refined moderately, which was also supported by the analytical data of **I**. Inversion of the structure provided no improvement in the refinement, which impeded further analysis. For **II**, the non-hydrogen atoms were refined anisotropically. Hydrogen atoms were included but not refined. The final cycle of the full-matrix least-squares refinement was based on the observed reflections ($I > 2\sigma(I)$) and converged with unweighted and weighted agreement factors of $R = \sum||F_o|-|F_c||/\sum|F_o|$ and $R_w = (\sum w(|F_o|-|F_c|)^2/\sum wF_o^2)^{1/2}$ as listed in Table 1. Plots of $\sum w(|F_o|-|F_c|)^2$ versus $|F_o|$, the reflection order in the data collection, sin $\theta/\lambda$ and various classes of indices showed no unusual trends. All calculations were performed using the teXsan crystallographic software package of Molecular Structure Corporation.[13] Tables giving atomic coordinates, equivalent isotropic thermal parameters, and anisotropic displacement parameters for **I** and **II** are deposited as Document No. 72029 at the Office of the Editor of Bull. Chem. Soc. Jpn. Crystallographic data have been deposited at the CCDC, 12 Union Road, Cambridge CB2 1EZ, UK and copies can be obtained on request, free of charge, by quoting the publication citation and the deposition numbers 127347-127348.

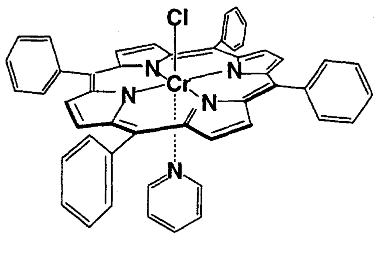

**[(tpp)CrCl(py)] (I)**

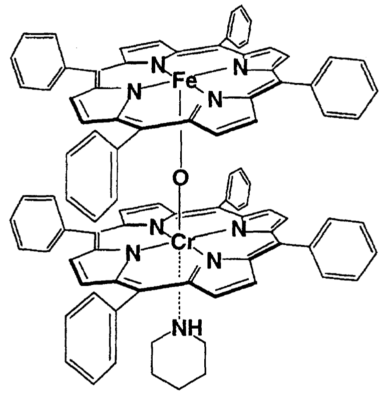

**[(tpp)FeOCr(tpp)(pip)] (II)**

Scheme 1.

## Results and Discussion

The preliminary X-ray study on [(ttp)FeOCr(tpp)(py)] (ttp = 5,10,15,20-tetra(*p*-methoxyphenyl)porphyrin dianion) reported by West et al.[8] revealed the presence of unresolved excess lattice solvent molecules and a difficulty to obtain crystals, which have impeded any refinement of the molecular structure. On the other hand, we found that single crystals of **II** with a piperidine molecule bound to the chromium atom can be easily obtained by recrystallization from benzene solutions after layering with diethyl ether. A considerable decay in the diffraction intensities noticed during the X-ray irradiation of **II** led us to use an imaging plate area detector for data collection, which allowed a satisfactory refinement of the structure. Analogous to [(ttp)FeOCr(tpp)(py)],[8] the UV spectrum of a solution prepared by dissolving **II** showed that **II** is hydrolyzed by traces of water to produce a solution containing **I**.[8,9b]

As a model for six-coordinate chromium(III), the mononuclear complex **I** was also subjected to crystallographic studies (Fig. 1). The Cr(1) atom in **I**, surrounded by the four coordinating nitrogen atoms of a porphyrin ring, extends only 0.045(1) Å above the best $N_4$ least-squares plane with a Cl(1)–Cr(1)–N(5) angle of 177.7(5)°. The arrangement around Cr(1) is pseudo octahedral. As for complex **II**, the Cr(1) atom extends 0.139(1) Å above the porphyrin plane with a O(1)–Cr(1)–N(9) angle of 179.5(2)° (Fig. 2). The CrOFe linkage is almost linear (177.7(3)°), which is similar to that of the structurally related [(py)(tpp)CrOFe(tmtaa)],[9b] where tmtaa is the dianion of 5,7,12,14-tetramethyldibenzo[*b*,*i*]-[1,4,8,11]tetraazacyclotetradeca-2,4,7,9,11,14-hexaene.

Table 1. Summary of X-Ray Crystallographic Data

| Complex | [(tpp)CrCl(py)]·$C_6H_{14}$ (**I**) | [(tpp)FeOCr(tpp)(pip)] (**II**) |
|---|---|---|
| Emp form | $C_{55}H_{47}N_5CrCl$ | $C_{93}H_{67}N_9OFeCr$ |
| Fw | 865.46 | 1434.45 |
| Cryst. syst. | Orthorhombic | Monoclinic |
| Space group | $P2_12_12_1$ (#19) | $P2_1/n$ (#14) |
| $a$/Å | 17.674(4) | 23.9233(9) |
| $b$/Å | 25.552(6) | 27.6178(6) |
| $c$/Å | 9.865(6) | 12.8707(5) |
| $\beta$/deg | | 105.6351(7) |
| $V$/Å$^3$ | 4455(2) | 8189.1(5) |
| $Z$ | 4 | 4 |
| Density (calcd)/g cm$^{-3}$ | 1.290 | 1.163 |
| Crystal size/mm | 0.2 × 0.2 × 0.3 | 0.3 × 0.2 × 0.03 |
| Radiation | Mo $K\alpha$ | Mo $K\alpha$ |
| Absn. coeff. $\mu$ | 3.61 cm$^{-1}$ | 3.61 cm$^{-1}$ |
| No. of reflns colld | 5716 | 10021 |
| No. of obsd reflns | 2791 ($I > 2.00\sigma(I)$) | 7617 ($I > 2.00\sigma(I)$) |
| Params | 593 | 946 |
| Refln./param. ratio | 5.04 | 8.05 |
| $R$ | 0.093 | 0.070 |
| $R_w$ | 0.090 | 0.085 |
| Goodness-of-fit | 1.99 | 1.32 |
| Max peak in diff map | 0.67 e$^-$ Å$^{-3}$ | 1.16 e$^-$ Å$^{-3}$ |
| Min peak in diff map | −0.30 e$^-$ Å$^{-3}$ | −0.34 e$^-$ Å$^{-3}$ |

Least-squares: Function minimized: $\sum w(|F_o|-|F_c|)^2$, where $w = (\sigma(F_o)^2+(0.020(F_o))^2)^{-1}$.

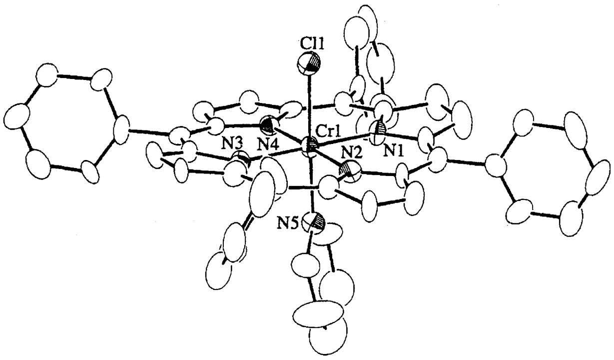

Fig. 1. ORTEP view (30% probability ellipsoids) of **I**. Non-carbon atoms are shown was shaded octants. The crystal solvent molecule (hexane) and hydrogen atoms are omitted for clarity. Selected bond lengths (Å) and angles (deg): Cr(1)–Cl(1), 2.294(4); Cr(1)–N(1), 2.027(8); Cr(1)–N(2), 2.032(10); Cr(1)–N(3), 2.053(9); Cr(1)–N(4), 2.039(9); Cr(1)–N(5), 2.12(1); Cl(1)–Cr(1)–N(5), 178.3(3).

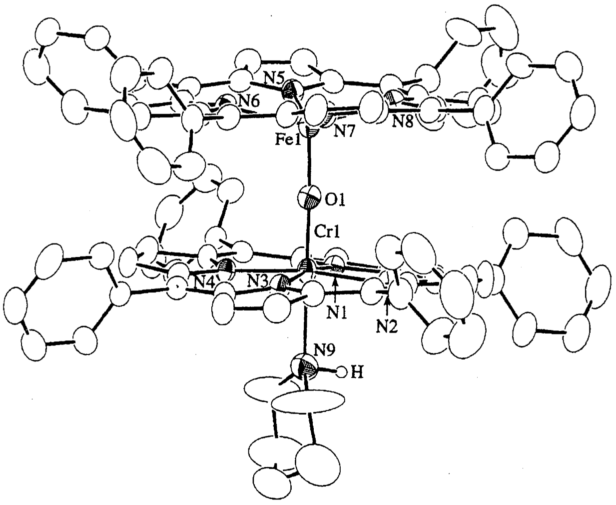

Fig. 2. ORTEP view (30% probability ellipsoids) of **II**. Non-carbon atoms are shown was shaded octants. Hydrogen atoms on carbons are omitted for clarity. Selected bond lengths (Å) and angles (deg): Cr(1)–O(1), 1.775(4); Cr(1)–N(1), 2.034(5); Cr(1)–N(2), 2.044(5); Cr(1)–N(3), 2.026(5); Cr(1)–N(4), 2.032(5); Cr(1)–N(9), 2.288(7); Fe(1)–O(1), 1.751(4); Fe(1)–N(5), 2.094(5); Fe(1)–N(6), 2.086(5); Fe(1)–N(7), 2.108(6); Fe(1)–N(8), 2.098(6); Fe(1)–O(1)–Cr(1), 177.7(3); O(1)–Cr(1)–N(9), 179.5(2).

It may be reasonable to suppose that the oxidation state of the chromium atom is reflected in the structure. The crystal structure of chromium porphyrins has been less studied than those of iron porphyrins. The structural data of **I** and **II**, combined with the previous studies,[14] allowed a rough diagnosis of the geometry around chromium in various oxidation states. Figure 3 shows the atomic arrangement around chromium for a series of isostructural families of chromium complexes with tpp ligands determined by crystallography, including those for **I** and **II**. It is obvious that chromium(IV) and chromium(V) are bound to axial ligands with significantly shorter distances than the lower valent chromium atoms (Fig. 3(a)). The extent of the deviation of the chromium atom from the porphyrin plane is more indicative of the oxidation state. It would be the preference of high valent chromium to be five coordinate rather than six that drives the deviation from the porphyrin plane. It appears that the deviation induces a

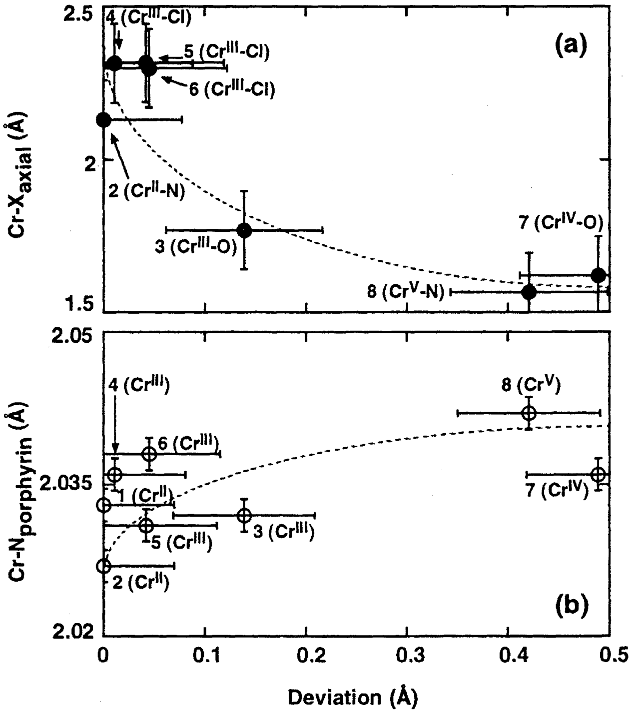

Fig. 3. Plots of deviations of Cr atoms from the porphyrin $N_4$ mean planes vs. (a) the distances between Cr and axial coordinating atoms ($X_{axial}$), and (b) the mean distances between Cr and porphyrin $N_4$ atoms for selected Cr(II, III, IV, and V) complexes with tpp ligands: 1, [(tpp)Cr$^{II}$]·(toluene)$_2$;[14a] 2, [(tpp)Cr$^{II}$(py)$_2$];[14b] 3, **II** (this work); 4, [(tpp)Cr$^{III}$Cl(1,2-Me$_2$-im)] (1,2-Me$_2$-im = 1,2-dimethylimidazole);[14c] 5, [(tpp)Cr$^{III}$Cl(1-Me-im)] (1-Me-im = 1-methylimidazole);[14c] 6, **I** (this work); 7, [(tpp)Cr$^{IV}$=O];[14d] 8, [(tpp)Cr$^{V}$≡N].[14e]

slight bond elongation between chromium and the equatorial nitrogen atoms (Fig. 3(b)).

A further important issue is the crystallographic confirmation of the proposed one electron transfer from iron(II) to oxochromium(IV) upon the formation of **II**.[8] The Fe(1) atom in **II**, lying as much as 0.536(1) Å above the porphyrin $N_4$ plane, and O(1) being 1.756(5) Å beyond the Fe(1) atom, represent a square-pyramidal coordination structure. Such a large metal deviation from the porphyrin plane is typically observed for μ-oxo diiron(III) complexes,[15] and is even larger than those of high-valent chromium complexes (Fig. 3). The disorder for the occupation of Fe and Cr atoms is denied not only by the coordination structure, which is fairly asymmetric with regard to the bridging μ-oxo bond, but also by the occupancies of two metal atoms calculated during the refinement of the structure. Accordingly, it can be concluded that piperidine is coordinated to chromium(III). The coordination environment around Cr(1) in **II** is fairly distorted from an octahedral arrangement. Nevertheless, it is clear from Fig. 3 that the structural features around Cr(1) are more like those of chromium(III) than those of chromium(IV).

Interest in the reactivity and structural properties of **II** derives from the crystallographically supported conclusion that, consistent with the spectroscopic properties,[8] complex **II** is an iron(III)–chromium(III) porphyrin, but the chromium(III) atom is substantially protruded from the porphyrin plane. The reactivity and structural changes that accompany the oxidation and reduction of **II** are currently under investigation.

We thank Dr. M. Shiro of Rigaku Corporation for his assistance in crystallography. This work was partially supported by the Grant-in-Aid for Scientific Research (Nos. 09555297, 09650982, 085344, and 11650878) and International Scientific Research Program (Joint Research No. 08044174) from the Ministry of Education, Science, Sports and Culture.

## References

1 a) K. Oyaizu and E. Tsuchida, *J. Am. Chem. Soc.*, **120**, 237 (1998). b) K. Yamamoto, K. Oyaizu, and E. Tsuchida, *J. Am. Chem. Soc.*, **118**, 12665 (1996). c) K. Oyaizu, K. Yamamoto, K. Yoneda, and E. Tsuchida, *Inorg. Chem.*, **35**, 6634 (1996).

2 a) K. Yamamoto, E. Tsuchida, M. Jikei, H. Nishide, and K. Oyaizu, *Macromolecules*, **26**, 3432 (1993). b) E. Tsuchida, K. Yamamoto, and K. Oyaizu, *J. Electroanal. Chem.*, **438**, 167 (1997).

3 K. Yamamoto, E. Shouji, H. Nishide, and E. Tsuchida, *J. Am. Chem. Soc.*, **115**, 5819 (1993).

4 E. Tsuchida, K. Yamamoto, K. Oyaizu, N. Iwasaki, and F. C. Anson, *Inorg. Chem.*, **33**, 1056 (1994).

5 D. -H. Chin, G. N. LaMar, and A. L. Balch, *J. Am. Chem. Soc.*, **102**, 4344 (1980).

6 R. J. Saxton, L. W. Olsen, and L. J. Wilson, *J. Chem. Soc., Chem. Commun.*, **1982**, 984.

7 a) S. Iwata, C. Ostermeier, B. Ludwig, and H. Michel, *Nature*, **376**, 660 (1995). b) T. Tsukihara, H. Aoyama, E. Yamashita, T. Tomizaki, H. Yamaguchi, K. Shinzawa-Itoh, R. Nakashima, R. Yaono, and S. Yoshikawa, *Science*, **269**, 1069 (1995).

8 D. J. Liston, B. J. Kennedy, K. S. Murray, and B. O. West, *Inorg. Chem.*, **24**, 1561 (1985).

9 a) C. T. Brewer and G. A. Brewer, *Inorg. Chem.*, **26**, 3420 (1987). b) P. J. Nichols, G. D. Fallon, B. Moubaraki, K. S. Murray, and B. O. West, *Polyhedron*, **12**, 2205 (1993).

10 a) D. A. Summerville, R. D. Jones, B. M. Hoffman, and F. Basolo, *J. Am. Chem. Soc.*, **99**, 8195 (1977). b) S. K. Cheung, C. J. Grimes, J. Wong, and C. A. Reed, *J. Am. Chem. Soc.*, **98**, 5028 (1976).

11 J. T. Groves, W. J. Kruper, Jr., R. C. Haushalter, and W. M. Butler, *Inorg. Chem.*, **21**, 1363 (1982).

12 L. M. Epstein, D. K. Straub, and C. Maricondi, *Inorg. Chem.*, **6**, 1720 (1967).

13 "teXsan: Crystal Structure Analysis Package," Molecular Structure Corporation (1985&1992).

14 a) W. R. Scheidt and C. A. Reed, *Inorg. Chem.*, **17**, 710 (1978). b) W. R. Scheidt, A. C. Brinegar, J. F. Kirner, and C. A. Reed, *Inorg. Chem.*, **18**, 3610 (1979). c) M. Inamo and K. Nakajima, *Bull. Chem. Soc. Jpn.*, **71**, 883 (1998). d) T. Ozawa and A. Hanaki, *Inorg. Chim. Acta*, **141**, 49 (1988). e) J. T. Groves, T. Takahashi, and W. M. Butler, *Inorg. Chem.*, **22**, 884 (1983).

15 a) B. Cheng, J. D. Hobbs, P. G. Debrunner, J. Erlebacher, J. A. Shelnutt, and W. R. Scheidt, *Inorg. Chem.*, **34**, 102 (1995). b) A. B. Hoffman, D. M. Collins, V. W. Day, E. B. Fleischer, T. S. Srivastava, and J. L. Hoard, *J. Am. Chem. Soc.*, **94**, 3620 (1972).